Dual-band Bandpass Filter Based on Two U-Shaped Defected Microstrip Structure

By Mussa Mabrok

Dual-band Bandpass Filter Based on Two U-Shaped Defected Microstrip Structure

Mussa Mabrok[1], Zahriladha Zakaria[2], Yully Erwanti Masrukin[3], Tole Sutikno[4]

Article Info

Article history:

Received Oct 1, 2018
Revised Dec 10, 2018
Accepted Jan 25, 2019

Keywords:

Dual-band
Bandpass filter
DMS
Wireless application
Microstrip filter

ABSTRACT

This paper presents design of dual-band bandpass filter by integrating conventional quarter-wavelength short circuit stubs bandpass filter with U-shaped defected microstrip structure notch filter. Based on the parametric analysis, it is found that high attenuation level can be achieved by using two U-shaped Defected Microstrip Structure separated by specific distance. The designed circuit simulated using advanced design system and fabricated based on Roger4350B. The simulation results are in good agreement with measured results. The designed filter covered two pass bands centered at 2.51 GHz and 3.59 GHz with 3-dB fractional bandwidth of 15.94 % and 15.86 %, respectively, return losses better than 15 dB, and insertion losses better than 1 dB. The designed device can be used for WLAN and WiMAX wireless communication applications.

Corresponding Author:

Zahriladha Zakaria,
Center for Telecommunication Research and Innovation (CeTRI),
Faculty of Electronics and Computer Engineering,
Universiti Teknikal Malaysia Melaka (UTeM),
Hang Tuah Jaya, 76100 Durian Tunggal, Melaka, Malaysia.
Email: zahriladha@utem.edu.my

1. INTRODUCTION

Microwave filters are needed in wireless communication systems to allow passing wanted signals and attenuate an unwanted signals. Previously, single-band filter which can only operates in single frequency band is used. To fulfil user end requirements, multi band microwave filter which can be supported in a single device are needed. A single device has capability to operate in multiple frequencies and support various wireless communication systems such as GSM, WLAN, and WiMAX is highly demanded [1-5]. To design multi-band bandpass filter (BPF), different approaches have been proposed in [6-21] to realize compact size and optimize the performance. However, they still suffer from some limitations such as high insertion loss as in [6,7,12], narrow bandwidth as in [17,19,20], and large size as in [16]. Therefore, to overcome the aforementioned problems and maintain a compact size. Integration of quarter-wavelength short-circuited stubs bandpass filter and U-shaped Defected Microstrip Structure (DMS) is proposed in the work. The proposed structure has many advantageous. First, BPF based on Quarter-wavelength short-circuit stubs can achieve wide bandwidths. Second, DMS does not occupy additional area as it is based on inserting slots into the microstrip line of BPF. The proposed design achieves two pass bands centered at 2.51 & 3.59 GHz with return loss better than 15 dB and insertion loss better than 1 dB. The design is verified by simulations using advanced design system (ADS) and measurements using vector network analyzer (VNA). Measured results are in good agreement with the simulated results.

2. RESEARCH METHOD

In this section, design of wideband BPF based on five sections quarter-wavelength (λ/4) short circuit stubs is presented, followed by designing U-shaped DMS notch filter. Then, integration of bandpass filter with U-shaped DMS to produce dual-band bandpass filter. Parametric analysis is conducted based on both the position and number of U-shaped DMS in order to assess the performance of the designed filter.

2.1. Wideband Bandpass Filter

Conventional microstrip BPF based on λ/4 short circuited stub is commonly used in the RF/Microwave applications [23]. First of all, the degree of the low pass prototype, N and the ratio of stopband and passband bandwidth, S is calculated using formula (2.1) and (2.2).

$$N \geq \frac{L_A + L_R + 6}{20\log_{10}[S + (S^2 - 1)^{1/2}]} \tag{2.1}$$

Where, L_A= Stopband insertion loss, L_R= Passband return loss. S = Ratio of stopband to passband bandwidth And the ratio of stopband and passband bandwidth can be calculate using equation (2.2);

$$S = \frac{Passband\ Bandwidth}{Stopband\ Bandwidth} = \frac{3.9}{2.3} = 1.696 \tag{2.2}$$

Therefore,

$$N \geq \frac{1 + 15 + 6}{20\log_{10}\left[1.696 + (1.696^2 - 1)^{\frac{1}{2}}\right]} = 4.78 \sim 5$$

The modeling circuit of the proposed wideband bandpass filter is illustrated in Figure 1. The model of bandpass filter comprises of 5th order shunt short stubs in length of λg/4 with the connecting lines. The λ_g is the guided wavelength in the medium of propagation at the mid-band frequency, f_0.

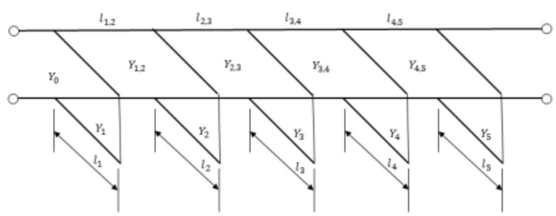

Figure 1. Modeling circuit of the proposed wideband bandpass filter

The specifications of wideband bandpass filter based on quarter-wavelength short circuit stubs are shown in Table 1.

Table 1. Bandpass filter specification for quarter wavelength short circuit stub

Bandpass Filter Specification	
Frequency Band	2.3 – 3.9 GHz
Fractional Bandwidth, *FBW*	51.61 %
Stopband Insertion Loss, L_A	0.3 dB
Passband Return Loss, L_R	> 20 dB

Based on the modeling circuit in Figure 1, all the obtained values of admittances and impedances for five short-circuited stubs (Y_i and Z_i) and transmission lines ($Y_{i,i+1}$ and $Z_{i,i+1}$) are tabulated in Table 2. The tabulated impedances and admittances can be calculated using the following equations:

$$\frac{J_{1,2}}{Y_0} = g_0\sqrt{\frac{hg_1}{g_2}} = (1)\sqrt{\frac{(2)(1.468)}{(1.3712)}} = 1.2933 \quad (2.3)$$

$$\frac{J_{2,3}}{Y_0} = \frac{hg_0g_1}{\sqrt{g_2g_3}} = \frac{(2)(1)(1.468)}{\sqrt{(1.3712)(1.9750)}} = 1.3937 \quad (2.4)$$

$$\frac{J_{3,4}}{Y_0} = \frac{hg_0g_1}{\sqrt{g_3g_4}} = \frac{(2)(1)(1.468)}{\sqrt{(1.9750)(1.3712)}} = 1.3937 \quad (2.5)$$

$$\frac{J_{4,5}}{Y_0} = \frac{hg_0g_1}{\sqrt{g_4g_5}} = \frac{(2)(1)(1.812)}{\sqrt{(1.5734)(2.0967)}} = 1.30067 \quad (2.6)$$

$$\frac{J_{5,6}}{Y_0} = \frac{hg_0g_1}{\sqrt{g_5g_6}} = \frac{(2)(1)(1.812)}{\sqrt{(2.0967)(1.4228)}} = 1.3677 \quad (2.7)$$

$$\frac{J_{6,7}}{Y_0} = g_0\sqrt{\frac{hg_1g_8}{g_0g_6}} = (1)\sqrt{\frac{(2)(1.1812)(1)}{(1)(1.4228)}} = 1.2886 \quad (2.8)$$

Where, $J_{i,i+1}$ is the J-inverter, h= 2 (dimensionless constant), and g_0 *to* g_8 are the element values for Chebyshev lowpass prototype filters.

To calculate Y_0, the $N_{1,2}$ have to be calculated first using equation (2.9):

$$N_{1,2} = \sqrt{\left(\frac{J_{1,2}}{Y_0}\right)^2 + \left(\frac{hg_0g_1\tan\theta}{2}\right)^2} = \sqrt{(1.2933)^2 + \left(\frac{(2)(1)(1.1468)\tan(1.1655)}{2}\right)^2} \quad (2.9)$$
$$= \sqrt{(1.2933)^2 + (7.1443)^2} = 2.9693$$

$$N_{2,3} = \sqrt{\left(\frac{J_{2,3}}{Y_0}\right)^2 + \left(\frac{hg_0g_1\tan\theta}{2}\right)^2} = \sqrt{(1.3937)^2 + \left(\frac{(2)(1)(1.1468)\tan(1.1655)}{2}\right)^2} \quad (2.10)$$
$$= \sqrt{(1.3937)^2 + (7.1443)^2} = 3.01441$$

$$N_{3,4} = \sqrt{\left(\frac{J_{3,4}}{Y_0}\right)^2 + \left(\frac{hg_0g_1\tan\theta}{2}\right)^2} = \sqrt{(1.3937)^2 + \left(\frac{(2)(1)(1.1468)\tan(1.1655)}{2}\right)^2} \quad (2.11)$$
$$= \sqrt{(1.3937)^2 + (7.1443)^2} = 2.42434$$

$$N_{4,5} = \sqrt{\left(\frac{J_{4,5}}{Y_0}\right)^2 + \left(\frac{hg_0g_1\tan\theta}{2}\right)^2} = \sqrt{(1.30067)^2 + \left(\frac{(2)(1)(1.1812)\tan(1.0472)}{2}\right)^2} \quad (2.12)$$
$$= \sqrt{(1.30067)^2 + (2.0459)^2} = 2.42434$$

$$N_{5,6} = \sqrt{\left(\frac{J_{5,6}}{Y_0}\right)^2 + \left(\frac{hg_0g_1\tan\theta}{2}\right)^2} = \sqrt{(1.3677)^2 + \left(\frac{(2)(1)(1.1812)\tan(1.0472)}{2}\right)^2} \quad (2.13)$$
$$= \sqrt{(1.3677)^2 + (2.0459)^2} = 2.46099$$

$$N_{6,7} = \sqrt{\left(\frac{J_{6,7}}{Y_0}\right)^2 + \left(\frac{hg_0g_1\tan\theta}{2}\right)^2} = \sqrt{(1.2886)^2 + \left(\frac{(2)(1)(1.1812)\tan(1.0472)}{2}\right)^2} \quad (2.14)$$
$$= \sqrt{(1.2886)^2 + (2.0459)^2} = 2.41787$$

Y_1 is the stubs admittances and can be calculate using equation (2.15):

$$Y_1 = g_0 Y_0 \left(1 - \frac{h}{2}\right) g_1 \tan\theta + Y_0 \left(N_{1,2} - \frac{J_{1,2}}{Y_0}\right) \quad (2.15)$$

$$= (1)\left(\frac{1}{50}\right)\left(1 - \frac{2}{2}\right)(1.1812)\tan(1.1655) + \left(\frac{1}{50}\right)(2.9693 - 1.2933)$$

$$= 0.03352$$

Y_i can be calculate using equation (2.16) for $i = 2\ to\ n$

$$Y_2 = Y_0 \left(N_{1,2} + N_{2,3} - \frac{J_{1,2}}{Y_0} - \frac{J_{2,3}}{Y_0}\right) = \left(\frac{1}{50}\right)(2.9693 + 3.01441 - 1.2933 - 1.3937) = 0.06593 \quad (2.16)$$

$$Y_3 = Y_0 \left(N_{2,3} + N_{3,4} - \frac{J_{2,3}}{Y_0} - \frac{J_{3,4}}{Y_0}\right) = \left(\frac{1}{50}\right)(3.01441 + 3.01441 - 1.3937 - 1.3937) \quad (2.17)$$

$$= 0.0648284$$

$$Y_4 = Y_0 \left(N_{3,4} + N_{4,5} - \frac{J_{3,4}}{Y_0} - \frac{J_{4,5}}{Y_0}\right) = \left(\frac{1}{50}\right)(2.42434 + 2.42434 - 1.30067 - 1.30067) \quad (2.18)$$

$$= 0.04495$$

$$Y_5 = Y_0 \left(N_{4,5} + N_{5,6} - \frac{J_{4,5}}{Y_0} - \frac{J_{5,6}}{Y_0}\right) = \left(\frac{1}{50}\right)(2.42434 + 2.46099 - 1.30067 - 1.36777) \quad (2.19)$$

$$= 0.04435$$

$$Z_i = \frac{1}{Y_i} \quad (2.20)$$

$Y_{i,i+1}$ can be obtained by using equation (2.21 to 2.24):

$$Y_{1,2} = Y_0 \left(\frac{J_{1,2}}{Y_0}\right) = \left(\frac{1}{50}\right)(1.2933) = 0.025866 \quad (2.21)$$

$$Y_{2,3} = Y_0 \left(\frac{J_{2,3}}{Y_0}\right) = \left(\frac{1}{50}\right)(1.3937) = 0.027874 \quad (2.22)$$

$$Y_{3,4} = Y_0 \left(\frac{J_{3,4}}{Y_0}\right) = \left(\frac{1}{50}\right)(1.3937) = 0.027874 \quad (2.23)$$

$$Y_{4,5} = Y_0 \left(\frac{J_{3,4}}{Y_0}\right) = \left(\frac{1}{50}\right)(1.30067) = 0.02601 \quad (2.24)$$

$$Z_{i,i+1} = \frac{1}{Y_{i,i+1}} \quad (2.25)$$

Table 2. Design parameter for 5th order stub bandpass filter with quarter-wavelength short-circuited stubs

i	Yi (mhos)	Zi (ohm)	Yi,i+1 (mhos)	Zi,i+1 (ohm)
1	0.03352	29.8329	0.025866	38.6608
2	0.06593	15.1666	0.027874	35.8757
3	0.06482	15.4253	0.027874	35.8757
4	0.04495	22.2469	0.02601	38.6608
5	0.04435	22.5479		

The Z_1 to Z_5 are defined as the characteristic impedances of the short-circuited stubs while the $Z_{1,2}$ to $Z_{4,5}$ are the characteristic impedances for the connecting lines. Z_0 = 50Ω is chosen as terminal impedance for the matching when connected to the SMA connector. Figure 2 shows the schematic of an ideal design of 5th order bandpass filter λg/4 short circuit stubs.

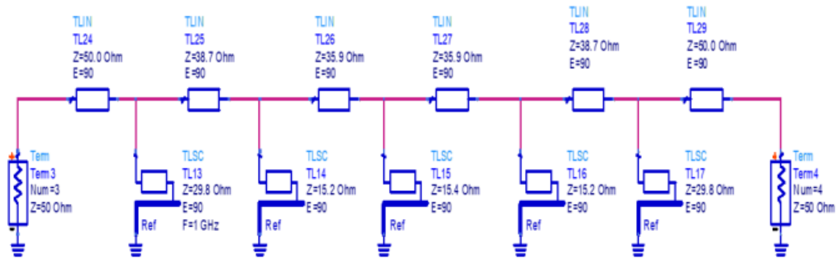

Figure 2. Ideal design of 5th order bandpass filter quarter-wavelength short-circuited stubs

Next, the ideal design in figure 2 is converted into microstrip design in figure 3 by automatically converting the characteristic impedance (Z) and electrical length (E) of each transmission line into width (W) and length (L) of the microstrip lines using LineCalc tool in Advanced Design System (ADS). Figure 3 shows the microstrip line design, where it is built based on Roger 4350 with dielectric constant, $\in_r$= 3.48, and thickness, h = 0.508 mm.

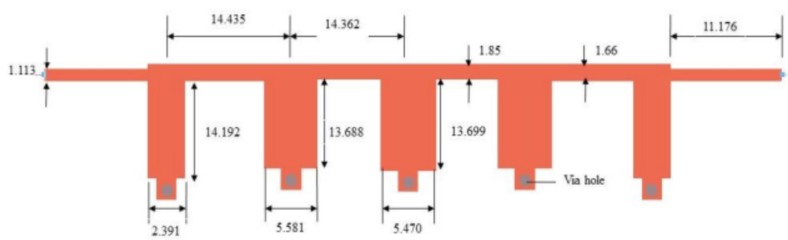

Figure 3. Microstrip bandpass filter based on five sections quarter-wavelength short circuit stubs

Figures 4(a), (b), and (c) show the effect of the length's stub on the resonance frequency of BPF. It can be observed that increasing the length's stubs will increase the return loss. The effect of the width's stubs is shown in figures 5(a), (b), and (c). For the first, second, fourth, and fifth's stubs. As we increase the width's stubs, the return loss at the resonance frequency increases. Whereas, increasing the middle (third) stub's width will lead to decreasing the return loss.

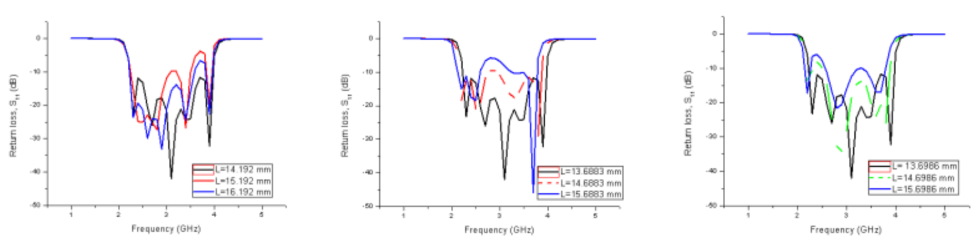

(a) (b) (c)

Figure 4. Parametric analysis on the effect of stub's length on the resonance frequency (a) 1st and 5th stub. (b) 2nd and 4th stub. (c) Middle stub.

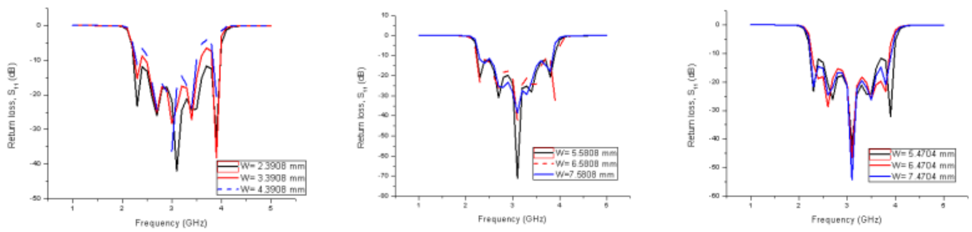

(a) (b) (c)

Figure 4. Parametric analysis on the effect of stub's width on the resonance frequency (a) 1st and 5th stub. (b) 2nd and 4th stub. (c) Middle stub.

Figure 5 (a) and (b) shows the simulation results of the designed ideal and microstrip filter respectively. Good agreement can be observed with slight difference due to the substrate's losses of the microstrip design. The simulated return loss (S_{11}) is better than 20 dB with insertion loss (S_{21}) of 0.01 dB over the frequency band 2.3-3.9 GHz. Furthermore, the designed filter yields high selectivity wideband response with fractional bandwidth (FBW) of 51.6 % at 3 GHz.

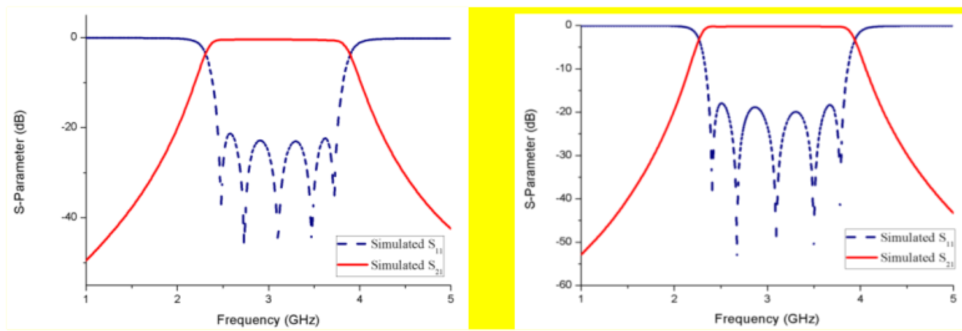

(a) (b)

Figure 5. (a) Simulation results of ideal five order conventional short circuit stubs bandpass filter. (b) Simulation results of microstrip five order conventional short circuit stubs bandpass filter.

2.2. Defected Microstrip Structure

In this section, DMS [24-25] is designed as a notch filter to subdivide the bandpass response into two passbands (dual-band). There are several types of DMS such as T-inversed shape, C-shape, and U-Shape. Based on our study in [26], U-shaped structure is the most suitable one due to its high selectivity and strong insertion loss. Therefore, it was selected to be integrated with BPF in order to produce dual-band BPF. The structure of U-shaped DMS is shown in figure 6. It comprises of horizontal and vertical slot in the middle of conductor line. In the center of the rectangular microstrip line is defected with U-shaped stub. The width and length of both branches of the U-shaped is indicated as l_2x h_2. Meanwhile, h_3 is stated as the detachment between the branches of the U-shaped. The lower section of the U-shaped is defected with the width of h_4. Figure 7 shows the simulation results of the U-shaped DMS. It achieves an attenuation level (S_{21}) better than -30 dB, return loss (S_{11}) of -0.2 dB at 3GHz.

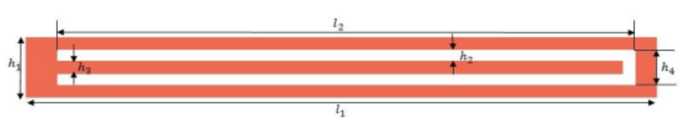

Figure 6. U-shaped DMS structure

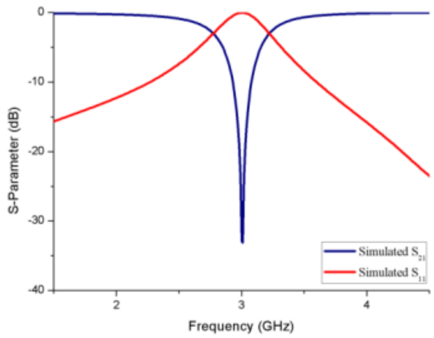

Figure 7. Simulation results of U-shaped DMS

3. INTEGRATION OF BANDPASS FILTER WITH U-SHAPED DMS

In order to produce dual-band BPF, U-shaped DMS is integrated with wideband BPF. Parametric study is carried out on the parameter of the number and position of U-shaped DMS filter as it is integrated within the wideband bandpass filter. The number and position of U-shaped DMS may affect the attenuation of the unwanted frequency band as it will be showed later in the following subsections. Table 3 shows the specifications of dual-band BPF.

Table 3. Specifications of dual-band bandpass filter

First Passband (GHz)	2.3-2.7
Second Passband (GHz)	3.1-3.9
Return Loss (dB)	<-20
Insertion Loss (dB)	<-1
Cantered Notch (GHz)	3.0

3.1. BPF with one U-shaped DMS

The integration between bandpass filter and one U-shaped DMS is shown in figure 8. Parametric analysis is done by varying the position of U-shaped DMS along the transmission line of bandpass filter. The position of d is varied from 16 to 26 mm with a step size of 5 mm. From figure 9, it can be observed that the distance d = 16 mm from the Port 1 attained good performance in terms of return loss, insertion loss, and attenuation.

3.2. BPF with two U-shaped DMS

In this section, two U-shaped DMS is integrated with bandpass filter in order to enhance the performance of the dual-band bandpass filter as shown in figure 10.

Figure 8. Proposed integrated of bandpass filter with one U-shaped DMS

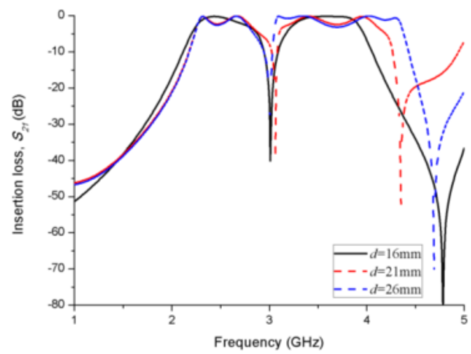

Figure 9. Effect of notch response as d is varied

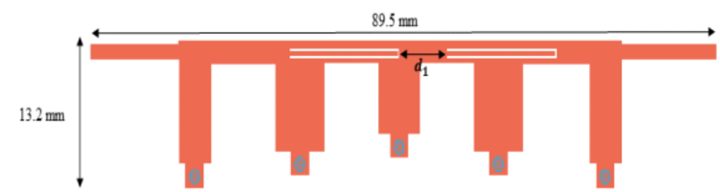

Figure 10. Bandpass filter with two U-shaped DMS

Figure 11 outlined the comparison of the simulated response of the designed bandpass filter with one DMS and two DMSs. It is identified that the notch response is 44 % improved with two DMSs at center frequency of 3 GHz with the attenuation level of 68 dB compared to one DMS. The simulated two passbands for two DMSs has been found to be at the center frequencies of 2.45 GHz and 3.6 GHz with the fractional bandwidth of 16% and 16.7% respectively. The simulated return and insertion losses are greater than 20 dB and better than 1 dB, respectively. It is Proven that the integration of two DMSs has enhanced the design response.

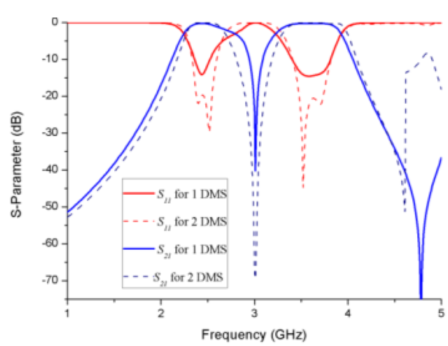

Figure 11. Performance comparison of simulated response of dual-band Bandpass filter with one and two DMSs

The integration of BPF with two U-shaped DMS is fabricated using Roger 4350B. The fabricated device occupied an area of 89.5 x 13.2 mm^2 as shown in figure 12.

Figure 12. Fabricated dual-band bandpass filter

Figure 13(a) presented the comparison between the simulated and fabricated response of dual-band bandpass filter. Good agreement can be observed between the simulated and measured results with slight deviation due to fabrication tolerance. The dual-band BPF operates at 2.51 GHz and 3.59 GHz with 3-dB fractional bandwidth of 15.94 % and 15.86 %, respectively. The measured return losses are better than 15 dB, while the measured insertion losses are better than 1 dB. Group delay for both simulated and measured response of dual-band bandpass filter is shown in Figure 11(b). The measured group delay is discovered quite flat and smooth in the overall band aside from the notch band.

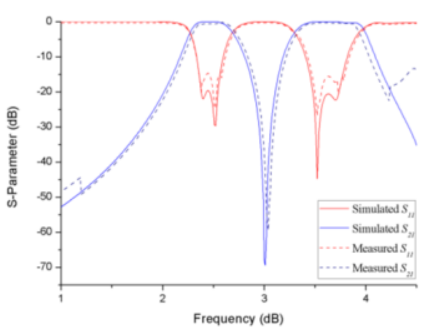

(a)

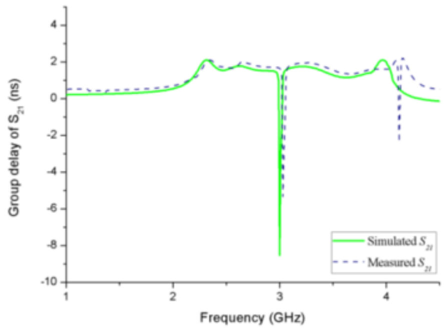

(b)

Figure 13. (a) Performance comparison between simulated and measured response of dual-band bandpass filter. (b) Comparison of group delay between simulated and measured response of dual-band bandpass filter

4. CONCLUSION

In conclusion, dual-band bandpass filter based on an integration of conventional short circuit stubs bandpass filter and two U-shaped DMS has been designed successfully. Advanced design system has been used to simulate the designed circuit. Roger 4350B board has been used to fabricate the designed filter. The design process started with designing five section quarter-wavelength short circuit stubs bandpass filter. Then, U-shaped DMS is designed as a band stop filter to produce a notch response at 3 GHz. Finally, an integration between U-shaped DMS and bandpass filter to produce dual-band response. Parametric analysis has been conducted on the position and number of U-shaped DMS to study their effect on the performance of dual-band BPF. As a result, two U-shaped DMS separated by distance d=16 mm showed an improvement in the notch response by 44 %. Where, 70 dB attenuation level has been achieved with two DMS, while 40 dB is achieved with one DMS at center frequency of 3 GHz. The proposed filter achieves two pass bands operated at 2.51 GHz and 3.59 GHz with 3-dB fractional bandwidths of 15.94 % and 15.86 %, respectively. Further study can be undertaken for triple-passband wide bandwidth with electronically tunable.

ACKNOWLEDGEMENTS

The authors gratefully acknowledge Universiti Teknikal Malaysia Melaka (UTeM) under the Zamalah Scheme for supporting this research work.